KINETIC AND MECHANISTIC STUDIES ON THE DECOMPOSITION OF NICKEL SALICYLATE

K. KISHORE and R. NAGARAJAN

High Energy Solids Laboratory, Indian Institute of Science, Bangalore 560012 (India)

(Received 14 March 1983)

ABSTRACT

Nickel salicylate has been prepared, characterized and its mode of thermal decomposition investigated by thermogravimetric analysis, differential thermal analysis and analysis of the intermediates. It was found from these studies that nickel salicylate decomposes by a three-step mechanism. The first step, in the temperature range 25–105°C, involves the loss of the water of crystallization, yielding the anhydrous material. The second step, in the temperature range 105–285°C is the loss of one of the salicylate ions, and the third and final step, in the temperature range 285–430°C, is the oxidation of this intermediate to the oxide. By following the rate of CO_2 evolution from the intermediates obtained after steps I and II of decomposition by mass spectral technique, the activation energies have been obtained. The activation energies for steps II and III were found to be 12 and 44 kcal $mole^{-1}$, respectively. While the former has been assigned to some physical process such as diffusion, the latter has been attributed to the process of Ni–O bond breakage.

INTRODUCTION

Metal salicylates (Msals) have potential application as additives in propellants [1] and in medicine [2]. In order to understand their role as additives, it is necessary to have a good understanding of their decomposition characteristics. Recently, the mechanism of the action of transition Msals in polymer combustion has been investigated [3]. A detailed mechanism for the decomposition of cobalt salicylate has also been reported recently [4]. In the present investigation, nickel salicylate (Nisal) has been synthesized, characterized and its mechanism of decomposition investigated. Studies on the kinetics of the decomposition of Nisal have also been carried out.

EXPERIMENTAL

Preparation

Saturated solutions of $Ni(NO_3)_2$ and Na salicylate were mixed at room temperature and the solution was kept overnight to obtain the product. The

TABLE 1

Results of Ni and salicylate estimations in nickel salicylate and its decomposition products

Compound	%Ni		%sal	
	Experi-mental	Expect-ed	Experi-mental	Expect-ed
Nickel salicylate	14.51 14.52	14.51	67.58 67.56	67.70
Residue after stage I	17.53 17.48	17.65	82.30 82.15	82.35
Residue after stage II	29.59 30.76	29.99	55.24 [a] 35.40 24.43	70.26

[a] The reason for the abnormally low values is explained in the text.

product thus obtained was washed several times with water and recrystallized from water to obtain green crystals of the complex.

Analyses

Estimation of Ni

Ni was estimated volumetrically using EDTA by the standard procedure [5]. The results are shown in Table 1.

Estimation of salicylate

Salicylate was estimated iodometrically by the method reported elsewhere [6]. The results are shown in Table 1.
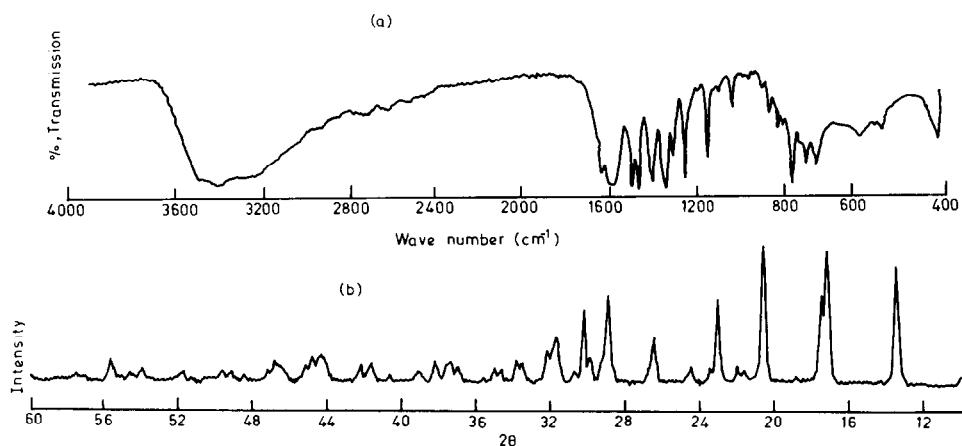

Fig. 1. (a) IR spectrum and (b) X-ray diffractogram of nickel salicylate.

X-Ray diffractometry

The X-ray diffractogram of the complex was taken on a Philips X-ray diffractometer with a PW 1050/70 vertical goniometer using $CuK\alpha$ radiation. The diffractogram is shown in Fig. 1.

IR spectrum

The IR spectrum of the complex was taken in KBr using a Carl–Zeiss UR-10 IR spectrophotometer. The spectrum is shown in Fig. 1.

Magnetic susceptibility measurements

The magnetic susceptibility measurements were made on an assembly described earlier [4]. The molar paramagnetic susceptibility of the complex was found to be 2.69 B.M.

Bomb calorimetry

The heat of combustion of anhydrous Nisal was determined using an all automatic Parr adiabatic bomb calorimeter equipped with a microprocessor.
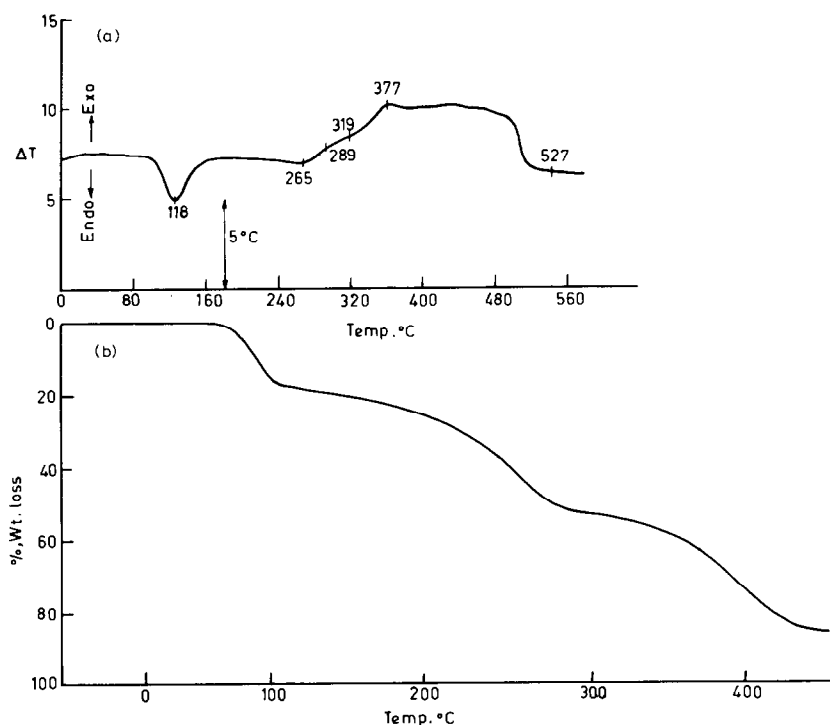

Fig. 2. TG and DTA traces of nickel salicylate. (a) Sample weight = 84.5 mg, heating rate = 10°C min^{-1}. (b) Sample weight = 7 mg, heating rate = 3°C min^{-1}.

Thermal studies

The thermogravimetric analysis (TG) of the complex was carried out in air on a Stanton-Redcroft model TG-750 thermobalance. A sample weight of 10 mg was used in each run and a heating rate of 10°C min^{-1} was employed. The TG is shown in Fig. 2.

The differential thermal analysis (DTA) of the complex, at a heating rate of 10°C min^{-1}, was carried out on an assembly [4] using about 85 mg of the sample. The DTA is shown in Fig. 2.

Mass spectral studies

The mass spectral studies were carried out on an MS10 mass spectrometer. The assembly used is shown in Fig. 3. The sample (1 mg) was taken in the thin-foiled Pt bucket. The bottom of the tube (A of Fig. 3) was kept in the middle of the furnace and allowed to stabilize at the experimental
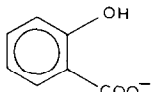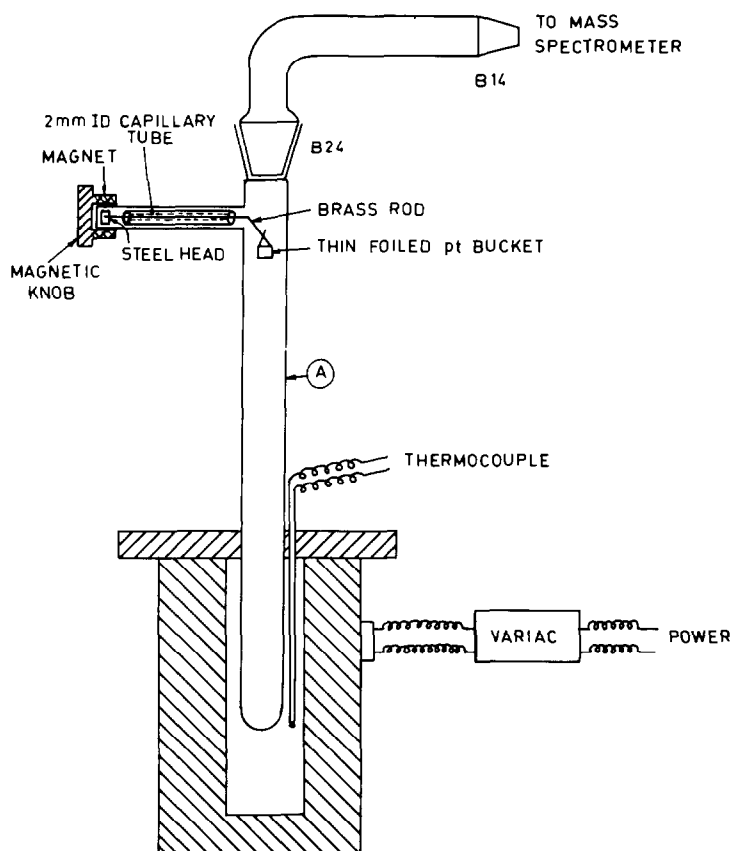

Fig. 3. The assembly used for mass spectral studies.

temperature for at least $\frac{1}{2}$ h. The sample was then dropped into the tube (along with the bucket) with the aid of the magnetic knob as follows: when the magnetic knob, shown near the steel head, is rotated, the rod inside the capillary also rotates causing the bucket containing the sample to fall inside the tube. The ion-current readings were taken from the instant of dropping the sample. The background CO_2 ion current was recorded before dropping the sample which was subtracted from the CO_2 ion-current values obtained for the sample.

RESULTS AND DISCUSSION

Structure

The estimations of Ni and salicylate show the formula of the complex to be $Ni(sal)_2(H_2O)_4$, where, sal = (a benzene ring with OH and COO^- substituents).

The fact that step I in TG is complete at 105°C shows that all four H_2O molecules are lattice waters. If the H_2O is co-ordinated, it should be eliminated at a higher temperature.

The phenolic O–H stretching frequency could not be seen clearly in the IR due to the presence of crystal water. However, the O–H bending at about 1340 cm^{-1} infers that the salicylate is bidentate. If the phenolic-O is unco-ordinated, the bending should occur at a higher frequency. The susceptibility measurement reveals that Ni is in state II. Based on the above observations, the structure of the complex is assigned as

(structural diagram of the Ni salicylate complex) $4\ H_2O$
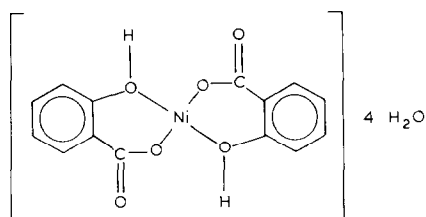
Thermal studies

The thermal decomposition of the Ni complex is similar to that of the Co complex reported earlier [4]. A summary of the results is as follows.

The TG of the complex shows that the decomposition occurs in three steps. Step I corresponds to loss of H_2O. This is evidenced by the estimation of Ni and salicylate in the residue obtained after step I. Besides, the weight loss tallies well with the proposed mode of decomposition (the expected

weight loss for the reaction, $[Ni(sal)_2] \cdot 4\,H_2O \rightarrow [Ni(sal)_2]$ is 17.79% and the experimentally obtained value is 16.2%).

Similarly, the estimation of Ni in the intermediate after the stage II and the weight loss from TG suggests that step II is nothing but the elimination of one of the salicylates from the anhydrous complex. (It may be noted that the residue obtained after stage II, unlike the other residue, was insoluble in H_2O or HCl. Dissolution had to be done in HNO_3 and it is clear from Table 1 that HNO_3 has oxidized a considerable amount of the salicylate, resulting in abnormally low values for salicylate. Hence, the proposition had to be made based on the estimation of Ni and the weight loss from TG alone). The reaction can be written as
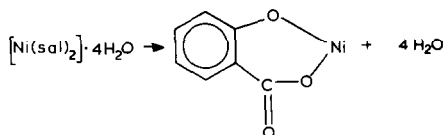

(The expected weight loss for the reaction of $[Ni(sal)_2] \cdot 4\,H_2O$ is 51.6% and the one obtained experimentally from TG is 48.0%.)

The fact that the final product is NiO is evidenced by X-ray studies. Thus, the third and final step is the oxidation of the residue from step II to form NiO.

When the decomposition was carried out on a glass assembly [7], deposits of needle-like crystals were observed on the sides of the tube as well as the strong smell of phenol. The needles were collected carefully by scraping the sides of the tube and analyzed using IR. The IR spectrum shows that the compound is nothing but salicylic acid (SA). The droplets collected at the bottom of the tube when tested with a solution of neutral $FeCl_3$ gave a violet coloration, suggesting the presence of phenol. It is evident that salicylic acid is produced due to the decomposition of the complex, which further decomposes to give phenol. When a similar analysis was carried out on the volatile products obtained during the third step, it was found that SA and phenol were also formed in this step.

The entire sequence of reactions can thus be written as
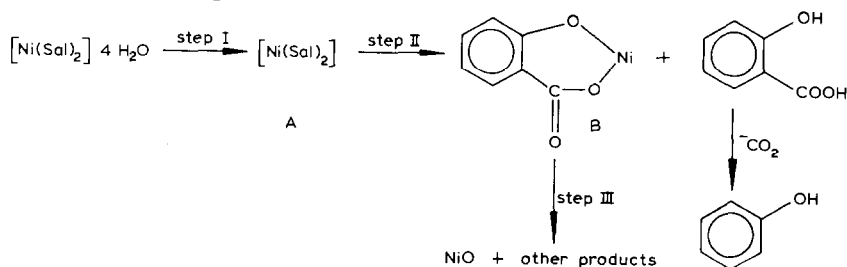
This mechanism has complementary support from the DTA of the complex. The endotherm around 110°C is due to loss of H_2O. The next broad and feeble endotherm around 260°C corresponds to the first salicylate loss. The

broad exotherm after this is due to the oxidation of the residue after step II. The small humps in this exotherm are due to side reactions as discussed earlier [4].

Kinetic studies

In order to probe further into the mechanism, kinetic studies were carried out using mass spectral technique. Since SA is formed both in steps II and III, which consequently decomposes to CO_2 and ϕ-OH, mass No. 44 (corresponding to CO_2) was monitored as a function of time for obtaining the kinetic data. In the experiment, a very thin-foiled Pt bucket weighing around 100 mg and containing about 1 mg sample was dropped into the decomposition tube pre-maintained at the desired isothermal temperature. The time
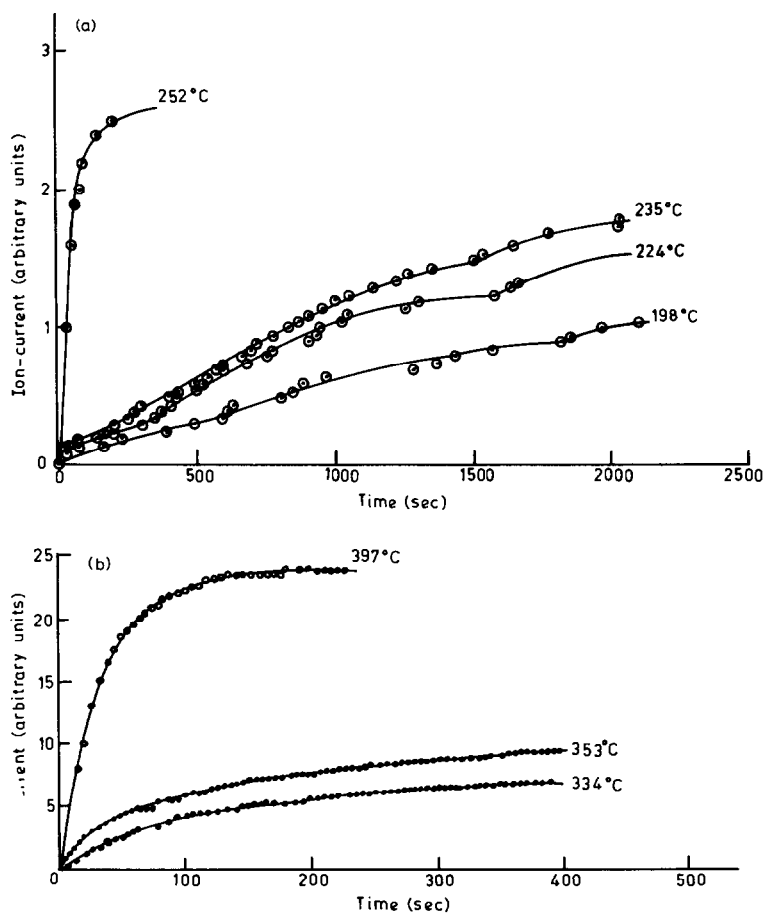

Fig. 4. Rate of CO_2 evolution by mass spectrometry. (a) 1 mg of anhydrous nickel salicylate. (b) 1 mg of the residue obtained after the second stage of the decomposition of nickel salicylate.

taken for the sample to attain the experimental temperature is very small and negligible as compared to the total reaction time. Thus, the error due to the decomposition of the sample prior to attaining the experimental temperature is minimal.

Figure 4 shows the growth of the CO_2 peak as a function of time for both the anhydrous salicylate(A) obtained after step I and the intermediate (B) obtained after step II. In Fig. 4, I^+T has to be plotted against time, as I^+T gives the quantitative measure of the species at temperature T But, as T is a constant during a run and as we are interested only in the time between two fractions of decomposition, I^+ has been plotted against time. It is quite evident that this will not affect the final result. Figure 4 shows humps in the curves of A at all temperatures. The reason for this may be as follows. Although the decomposition was carried out on the anhydrous sample, there is a likelihood that it absorbs a small amount of H_2O during the experimental operation. Thus, when the decomposition starts, two compounds are decomposing: (i) a small amount of the hydrated salicylate, and (ii) the rest, the anhydrous salicylate. The hydrated salicylate will also evolve CO_2, besides H_2O, as the temperatures are about 200°C and more. The rate of CO_2 evolution from the hydrated salicylate will be different from that of the anhydrous one. Hence, in the plot, the first hump corresponds to CO_2 evolution from the hydrated sample and the second is due to CO_2 evolution from A. That the first hump is due to CO_2 evolution from the hydrated salicylate is evidenced from the amount of CO_2—as only a small amount of the sample becomes hydrated, only a small amount of CO_2 is evolved.

Similarly, the third hump is due to CO_2 evolution from the residue (B) produced due to the decomposition of A. In the case of the mass spectra of B no hump is seen, which is obviously because this step involves only a one-step decomposition, viz. the oxidation of B to form NiO. Activation energy (E) calculations were made from the data presented in Fig. 4 using the method of Jacobs and Kureishy [8], considering the time taken for CO_2 evolution between the ion-current values 0.4 and 0.88. The reasons for choosing the ion-current values between 0.4 and 0.88 are as follows. The decomposition of the anhydrous sample occurs in the middle hump of curve A (Fig. 4). By choosing ion-current values between 0.4 and 0.88, all the three curves at different temperatures were covered. If we go for higher ion-current values (beyond 0.88) the curves at some temperature will be left out in the rate calculation and similarly, if lower ion-current values are taken (lower than 0.4) then the first hump corresponding to the evolution of CO_2 from the hydrated compound will be included, which is not required. Thus, the kinetic calculations consider only the decomposition of the anhydrous salicylate (A) to form the intermediate (B) which is produced after step I, as has been shown in the mechanism earlier. The E calculations yielded a value of 12 kcal mole^{-1}, which cannot be attributed to any bond breakage process. The intermediate (B) proposed to be formed after the second step can be formed

only by breakage of the Ni–O bond to remove one salicylate. If E corresponds to the bond breakage process, then it should be much higher than 12 kcal mole^{-1}. The E value obtained thus seems to correspond to some physical process. Intermediate A on decomposition gives B and salicylic acid which in turn decomposes to give ϕ-OH and CO_2. It is likely that CO_2 remains trapped in the solid and has to come to the surface by the process of diffusion. Thus, in step II, the bond breakage seems to be a faster process and the evolved CO_2, which has to come out of the solid by diffusion, seems to be the slower process and the rate controlling step although the exact mechanism is not known at present. However, at higher temperatures, when the solid matrix becomes porous due to the evolution of CO_2, the third and final step is associated with a faster rate of CO_2 escape from the solid and the rate controlling step becomes the bond breakage process. Calculation of E of the third step was again carried out using the Jacobs–Kureishy method [8] between the ion-current values 1 and 7. Here again, the ion-current values were chosen between 1 and 7 to include all three curves at different temperatures in the calculation of E. If, for similarity to the calculation done for the anhydrous sample (A), the ion-current values are chosen between 0.4 and 0.88, the region will be too small owing to the fast rate of decomposition at these temperatures. Here, as expected, the E value (44 kcal mole^{-1}) was much higher than that obtained for the second step. The Ni–O bond energy in complexes such as acetylacetonates, benzoyl acetonates, etc. has been reported in the literature to be between 44 and 56 kcal mole^{-1} [9]. In addition to this, we tried to calculate in the present work the Ni–O bond energy in Nisal using the heat of combustion data ($\Delta H_c = 1410.7$ kcal mole^{-1}) from calorimetry. The heat of vaporization of Nisal is required for the calculation, which is not available in the literature. Hence, as an approximation, the reported heat of vaporization of bis(salicyladehydrato)nickel(II) was substituted in the place of the heat of vaporization of Nisal, owing to the close similarity in structure between SA and salicylaldehyde ($\Delta H_{gasification} = 20.4$ kcal mole^{-1}) [10].

The value thus obtained for the Ni–O bond energy was 32 kcal mole^{-1}. The agreement is not very good as this is only a rough estimate. However, the order of magnitude is quite comparable. (Note: the heat of combustion measurements were made with anhydrous sample.) Thus, it is quite reasonable and justified to attribute the obtained E value of 44 kcal mole^{-1} to the Ni–O bond energy in the complex. Thus, the rate controlling step in the third and final step can be assigned to the Ni–O bond breakage process.

REFERENCES

1 M. Farber and R.D. Srivastava, Combust. Flame, 31 (1978) 309.
2 M. Weselowsky, Thermochim. Acta, 31 (1979) 133.

3 K. Kishore, G. Prasad and R. Nagarajan, J. Fire Flammability, 10(4) (1979) 269.

4 K. Kishore and R. Nagarajan, J. Therm. Anal., 22 (1981) 25.

5 A.I. Vogel, A Textbook of Quantitative Inorganic Analysis, The English Language Book Society and Longmans, London, 1975, pp. 435–436.

6 Chem. Abstr., 17 (1923) 6154.

7 K. Kishore, V.R. Pai Verneker, M.R. Sunitha and G. Prasad, Fuel, 56 (1977) 347.

8 P.W.M. Jacobs and A.R.T. Kureishy, J. Chem. Soc., (1964) 4718.

9 W. Kakolowicz and E. Giera, Thermochim. Acta, 32 (1–2) (1979) 19.

10 J.L. Wood and M.M. Jones, J. Phys. Chem., 67 (1963) 1049.